

Beam normal spin asymmetry in the quasi-RCS approximation

M. Gorchtein^{1,2}

¹*Genoa University, Department of Physics, 16146 Genoa, Italy*

²*California Institute of Technology, Pasadena, CA 91125, USA**

The two-photon exchange contribution to the single spin asymmetries with the spin orientation normal to the reaction plane is discussed for elastic electron-proton scattering in the equivalent photon approximation. In this case, hadronic part of the two-photon exchange amplitude describes real Compton scattering (RCS). We show that in the case of the beam normal spin asymmetry, this approximation selects only the photon helicity flip amplitudes of RCS. At low energies, we make use of unitarity and estimate the contribution of the πN multipoles to the photon helicity flip amplitudes. In the Regge regime, QRCS approximation allows for a contribution from two pion exchange, and we provide an estimate of such contributions. We furthermore discuss the possibility of the quark and gluon GPD's contributions in the QRCS kinematics.

PACS numbers: 12.40.Nn, 13.40.Gp, 13.60.Fz, 14.20.Dh

I. INTRODUCTION

Recently, the new polarization transfer data for the electromagnetic form factors ratio G_E/G_M [1] raised a lot of interest for the two photon exchange (TPE) physics in elastic electron proton scattering. These new data appeared to be incompatible with the Rosenbluth data [2]. A possible way to reconcile the two data sets was proposed [3], which consists in a more precise account on the TPE amplitude, the real part of which enters the radiative corrections to the cross section (Rosenbluth) and the polarization cross section ratio in a different manner. At present, only the IR divergent part of the two photon exchange contribution, corresponding to one of the exchanged photon being soft, is taken into the experimental analysis [4]. Two model calculations exist for the real part of the TPE amplitude [5, 6], and they qualitatively confirm that the exchange of two hard photons may be responsible for this discrepancy. In order to extract the electric form factor in the model independent way, one has thus to study the general case of Compton scattering with two spacelike photons. These two photon contributions are important for the electroweak sector, as well.

In view of this interest, parity-conserving single spin asymmetries in elastic ep -scattering with the spin orientation normal to the reaction plane regain an attention. These observables are directly related to the imaginary part of the TPE amplitude and have been an object of theoretical studies in the 1960's and 70's [7]. By analyticity, the real part of the TPE amplitude is given by a dispersion integral over its imaginary part. Therefore, a good understanding of this class of observables is absolutely necessary. Recently, first measurements of the beam normal spin asymmetry B_n ¹ have been performed

in different kinematics [8].

Though small (several to tens ppm), this asymmetry can be measured with a precision of fractions of ppm. Before implementing different models for the real part, where an additional uncertainty comes from the dispersion integral over the imaginary part, one should check the level of understanding of the imaginary part of TPE. These checks have been done for the existing data. Inclusion of the elastic (nucleon) intermediate state only [9] led to negative asymmetry of several ppm in the kinematics of SAMPLE experiment but was not enough to describe the data. The description of the beam normal spin asymmetry within a phenomenological model which uses the full set of the single pion electroproduction [10] did not give satisfactory description at any of the available kinematics. Especially intriguing appears the situation with the SAMPLE data with electron lab energy $E_{lab} = 200$ MeV, which is just above the pion production threshold where the theoretical input is well understood. On the other hand, an EFT calculation without dynamical pions [11] was somewhat surprisingly very successful in describing this kinematics for B_n . This success suggests that to the given order of chiral perturbation theory, the role of the dynamical pions for this observable might be not too large. Finally, a recent calculation within the leading logarithm approximation appeared, where only few dominant multipoles were used as input [12]. Surprisingly, the authors of [12] were able to describe all the experimental data at very different beam energies and scattering angles, while the full calculation of [10] failed to describe any of them.

Though even at low energies the situation with the imaginary part of TPE amplitude is by far not clear, an attention has to be paid to high energies, as well, since the dispersion integral which would give us its real part, should be performed over the full energy range. Due to relative ease of measuring B_n within the framework of parity violating electron scattering, new data from running and upcoming experiments [13] will stimulate further theoretical investigations of this new observable. A calculation of B_n in hard kinematics regime

*Electronic address: gorshtey@caltech.edu

¹ In the literature, also the A_n notation for beam normal spin asymmetry or vector analyzing power was adopted.

at high energy and momentum transfer was performed recently in the framework of generalized parton distributions (GPD's) and resulted in asymmetries of ~ 1.5 ppm. [14].

Since a ppm effect measurement at high momentum transfers is an extremely complicated task, the forward kinematics seems more favorable. For this kinematics, a calculation exists [15], where an observation is made that the contribution of the situation where the exchanged photons are nearly real and overtake the external electron kinematics is enhanced as $\ln^2(-t/m^2) \sim 100$, with m the electron mass and $t < 0$ the elastic momentum transfer. Making use of the optical theorem, the authors obtained estimates of B_n in this kinematics as large as 25-35 ppm. The calculation of [16] appeared afterwards showed that this result is not adequate, since the squared log term can only contribute with the Compton scattering amplitudes with the photon helicity flip. Indeed, this conclusion was confirmed in Ref. [17], the corrected version of [15]. It was noticed that the $\ln^2(-t/m^2)$ term should vanish in the forward kinematics due to gauge invariance, and the leading term is governed by a single (though still large) log term, $\ln(-t/m^2) \sim 10$. The predictions for B_n shifted correspondingly to $\approx -(4-6)$ ppm and agree with the preliminary data from HAPPEX experiment [13].

In order to provide an estimate of B_n , we use the equivalent photon or quasi-real Compton scattering approximation which is caused by the hard collinear kinematics, responsible for this $\ln^2(-t/m^2)$ enhancement. In this approximation, the leading contribution comes from the kinematical region with both exchanged photons are almost real. The hadronic tensor is taken at this kinematical point and can be taken out of the integration. For the hadronic tensor, we adopt the most general real Compton scattering amplitude and demonstrate that the contribution of the cross section (i.e., photon helicity conserving amplitudes) vanishes in the QRCS approximation. The remaining contributions are related to the photon helicity flip amplitudes. We provide the calculation of B_n at low energies, where πN intermediate states are expected to be the dominant contributions. In this kinematics, the asymmetry can be related to the pion photoproduction multipoles, and we discuss the relative contributions of different multipoles. At higher energies, we discuss forward kinematics, that is Regge regime, and note that the combinations of the RCS amplitudes appearing in the expression of B_n are related to 2π exchange in the t -channel. We provide an estimate of such a contribution but conclude that these are negligibly small. We furthermore discuss the hard regime and discuss possible contributions which might be enhanced by the large logarithms originating from the QRCS kinematics.

The article is organized as follows: in Section II, we define the kinematics, general ep -scattering amplitude and the observables of interest; in Section III, the two photon exchange mechanism and the photons kinematics is studied; the equivalent photons or quasi real Compton scattering approximation and its implementation for the

case of B_n is given in Section IV; we present our results in Section V and conclude with a short summary.

II. ELASTIC ep -SCATTERING AMPLITUDE

In this work, we consider elastic electron-proton scattering process $e(k) + p(p) \rightarrow e(k') + p(p')$ for which we define:

$$\begin{aligned} P &= \frac{p + p'}{2} \\ K &= \frac{k + k'}{2} \\ q &= k - k' = p' - p, \end{aligned} \quad (1)$$

and choose the invariants $t = q^2 < 0^2$ and $\nu = (P \cdot K)/M$ as the independent variables. M denotes the nucleon mass. They are related to the Mandelstam variables $s = (p + k)^2$ and $u = (p - k')^2$ through $s - u = 4M\nu$ and $s + u + t = 2M^2$. For convenience, we also introduce the usual polarization parameter ε of the virtual photon, which can be related to the invariants ν and t (beglecting the electron mass m):

$$\varepsilon = \frac{\nu^2 - M^2\tau(1 + \tau)}{\nu^2 + M^2\tau(1 + \tau)}, \quad (2)$$

with $\tau = -t/(4M^2)$. Elastic scattering of two spin $1/2$ particles is described by six independent amplitudes. Three of them do not flip the electron helicity [3],

$$\begin{aligned} T_{no\ flip} &= \frac{e^2}{-t} \bar{u}(k') \gamma_\mu u(k) \\ &\cdot \bar{u}(p') \left(\tilde{G}_M \gamma^\mu - \tilde{F}_2 \frac{P^\mu}{M} + \tilde{F}_3 \frac{K P^\mu}{M^2} \right) u(p), \end{aligned} \quad (3)$$

while the other three are electron helicity flipping and thus have in general the order of the electron mass m [14]:

$$\begin{aligned} T_{flip} &= \frac{m}{M} \frac{e^2}{-t} \left[\bar{u}(k') u(k) \cdot \bar{u}(p') \left(\tilde{F}_4 + \tilde{F}_5 \frac{K}{M} \right) u(p) \right. \\ &\left. + \tilde{F}_6 \bar{u}(k') \gamma_5 u(k) \cdot \bar{u}(p') \gamma_5 u(p) \right] \end{aligned} \quad (4)$$

In the one-photon exchange (Born) approximation, two of the six amplitudes match with the electromagnetic form factors,

$$\begin{aligned} \tilde{G}_M^{Born}(\nu, t) &= G_M(t), \\ \tilde{F}_2^{Born}(\nu, t) &= F_2(t), \\ \tilde{F}_{3,4,5,6}^{Born}(\nu, t) &= 0 \end{aligned} \quad (5)$$

² In elastic ep -scattering, the usual notation for the momentum transfer is $Q^2 = -q^2$ but we prefer the more general notation t to avoid confusion with the incoming and outgoing photon virtualities in forward doubly virtual Compton scattering we will be concerned in the following.

where $G_M(t)$ and $F_2(t)$ are the magnetic and Pauli form factors, respectively. For further convenience we define also $\tilde{G}_E = \tilde{G}_M - (1 + \tau)\tilde{F}_2$ and $\tilde{F}_1 = \tilde{G}_M - \tilde{F}_2$ which in the Born approximation reduce to electric form factor G_E and Dirac form factor F_1 , respectively. For a beam polarized normal to the scattering plane, one can define a single spin asymmetry,

$$B_n = \frac{\sigma_\uparrow - \sigma_\downarrow}{\sigma_\uparrow + \sigma_\downarrow}, \quad (6)$$

where σ_\uparrow (σ_\downarrow) denotes the cross section for an unpolarized target and for an electron beam spin parallel (antiparallel) to the normal polarization vector defined as

$$S_n^\mu = \left(0, \frac{[\vec{k} \times \vec{k}']}{|\vec{k} \times \vec{k}'|} \right), \quad (7)$$

normalized to $(S \cdot S) = -1$. Similarly, one defines the target normal spin asymmetry A_n . It has been shown in the early 1970's [7] that such asymmetries are directly related to the imaginary part of the T -matrix. Since the electromagnetic form factors and the one-photon exchange amplitude are purely real, B_n obtains its finite contribution to leading order in the electromagnetic constant α_{em} from an interference between the Born amplitude and the imaginary part of the two-photon exchange amplitude. In terms of the amplitudes of Eqs.(3,4), the beam normal spin asymmetry is given by:

$$B_n = -\frac{m}{M} \sqrt{2\varepsilon(1-\varepsilon)} \sqrt{1+\tau} (\tau G_M^2 + \varepsilon G_E^2)^{-1} \cdot \left\{ \tau G_M \text{Im}\tilde{F}_3 + G_E \text{Im}\tilde{F}_4 + F_1 \frac{\nu}{M} \text{Im}\tilde{F}_5 \right\}. \quad (8)$$

For completeness, we also give here the expression of target normal spin asymmetry T_n ³ in terms of invariant amplitudes:

$$T_n = \sqrt{2\varepsilon(1+\varepsilon)} \sqrt{\tau} (\tau G_M^2 + \varepsilon G_E^2)^{-1} \cdot \left\{ (1+\tau) \left[F_1 \text{Im}\tilde{F}_2 - F_2 \text{Im}\tilde{F}_1 \right] + \left(\frac{2\varepsilon}{1+\varepsilon} G_E - G_M \right) \frac{\nu}{M} \text{Im}\tilde{F}_3 \right\}. \quad (9)$$

III. TWO PHOTON EXCHANGE

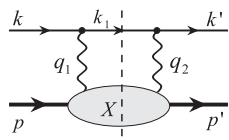


FIG. 1: Two-photon exchange diagram.

The imaginary part of the two-photon exchange (TPE) graph in Fig.1 is given by

$$\text{Im}\mathcal{M}_{2\gamma} = e^2 \int \frac{|\vec{k}_1|^2 d|\vec{k}_1| d\Omega_{k_1}}{2E_1(2\pi)^3} \bar{u}' \gamma_\nu (\vec{k}_1 + m) \gamma_\mu u \cdot \frac{1}{Q_1^2 Q_2^2} W^{\mu\nu}(w^2, Q_1^2, Q_2^2), \quad (10)$$

where $W^{\mu\nu}(w^2, Q_1^2, Q_2^2)$ is the imaginary part of doubly virtual Compton scattering tensor. Q_1^2 and Q_2^2 denote the virtualities of the exchanged photons in the TPE diagram, and w is the invariant mass of the intermediate hadronic system. We next study the kinematics of the exchanged photons. Neglecting the small electron mass and using the c.m. frame of the electron and proton, one has:

$$Q_{1,2}^2 = 2|\vec{k}| |\vec{k}_1| (1 - \cos \Theta_{1,2}), \quad (11)$$

with $|\vec{k}| = \frac{s-M^2}{2\sqrt{s}} \equiv k$ the three momentum of the incoming (and outgoing) electron, $|\vec{k}_1| = \sqrt{(\frac{s-w^2+m^2}{2\sqrt{s}})^2 - m^2}$ that of the intermediate electron, and $\cos \Theta_2 = \cos \Theta \cos \Theta_1 + \sin \Theta \sin \Theta_1 \cos \phi$. The kinematically allowed values of the virtualities of the exchanged photons (the restriction is due to the fact that the intermediate electron is on-shell) are represented by the internal area of the ellipses shown in Fig. 2. The ellipses are drawn

Accessible values of Q_1^2, Q_2^2

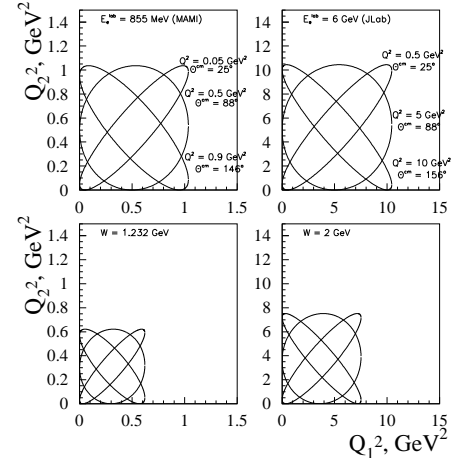


FIG. 2: Kinematically allowed values of the photon virtualities $Q_{1,2}^2$.

inside a square whose side is defined through the external kinematics (k) and the invariant mass of the intermediate hadronic state (w^2 or k_1), while the form solely by the scattering angle. If choosing higher values of the mass of the hadronic system $w^2 < s$, it leads to scaling the size of the ellipse by a factor of $\frac{s-w^2}{s-M^2}$. In the limit

³ Also A_n notation for target normal spin asymmetry exists in the literature.

$w^2 = (\sqrt{s} - m_e)^2$, the ellipses shrink to a point at the origin and both photons are nearly real. This is not a soft photon (IR) singularity, however, since the real photons' energy remains large enough in order to provide the transition from nucleon with the mass M to the intermediate state X with the mass w . Instead, the intermediate electron is soft, $k_1^\mu \approx (m_e, \vec{0})$, therefore this kind of kinematics does not lead to an IR divergency which can only occur if the intermediate hadronic state is the nucleon itself. In the following we are going to study this kinematical situation in more detail.

IV. QUASI-RCS APPROXIMATION

We consider the kinematical factors under the integral over the electron phase space of Eq.(10) at the upper limit of the integration over the invariant mass of the intermediate hadronic state, $w \rightarrow \sqrt{s} - m_e$:

$$\frac{\vec{k}_1^2}{E_1} \frac{1}{Q_1^2 Q_2^2} \sim \frac{1}{4k^2 E_1} \sim \frac{1}{m} \frac{1}{4k^2}, \quad (12)$$

In this range of the hadronic mass w , the exchanged photons are real, and the contribution of real Compton scattering (RCS) to the 2γ -exchange graph is enhanced by a factor of $1/m$ (it is not a singularity since B_n has a factor of m in front).

We next rewrite the contraction of the hadronic and the leptonic tensors in Eq.(10) identically as

$$\begin{aligned} l_{\mu\nu} W^{\mu\nu}(W^2, Q_1^2, Q_2^2) &= l_{\mu\nu}^{(0)} W^{\mu\nu}(s, 0, 0) \\ &+ l_{\mu\nu}^{(1)} W^{\mu\nu}(s, 0, 0) \\ &+ l_{\mu\nu} [W^{\mu\nu}(W^2, Q_1^2, Q_2^2) - W^{\mu\nu}(s, 0, 0)], \end{aligned} \quad (13)$$

where we expanded the leptonic tensor $l_{\mu\nu} = l_{\mu\nu}^0 + l_{\mu\nu}^1$ with

$$\begin{aligned} l_{\mu\nu}^0 &= m\bar{u}'\gamma_\nu\gamma_\mu u \\ l_{\mu\nu}^1 &= \bar{u}'\gamma_\nu\cancel{k}_1\gamma_\mu u. \end{aligned} \quad (14)$$

In Eq.(13), only the first term does not vanish in the QRCS limit, while the second and third are at least linear in k_1 . In the limit $W^2 \rightarrow s$, one has $\cancel{k}_1 \rightarrow m\gamma_0$, which is to be compared to the term $m \cdot 1$ in $l_{\mu\nu}^0$. Though on the first glance on the first glance they are of the same order, the additional γ -matrix picks an extra electron mass m from one of the projectors $\cancel{k} + m$ when performing the summation over electron spins. Quasi-real Compton scattering (QRCS) approximation consists in assuming the first term to be dominant due to the kinematical enhancement under the integral and in neglecting the second one. In general, this kind of contributions coming from QRCS kinematics will always be present in the full calculation, since the second term in Eq.(13) is constructed in such a way that the resulting integral is regular at the QRCS point. In the following, the QRCS approximation will be used. Hence, the hadronic tensor can be taken out of the

integration over the electron phase space. The remaining integral is

$$I_0 = \int \frac{d^3 \vec{k}_1}{2E_1(2\pi)^3} \frac{1}{Q_1^2 Q_2^2}, \quad (15)$$

The result of the integration reads:

$$I_0 = \frac{1}{-32\pi^2 t} \left\{ \ln^2 \left(\frac{-t}{m^2} \frac{E_{thr}^2}{E^2} \right) + 8Sp \left(\frac{E_{thr}}{E} \right) \right\}, \quad (16)$$

where $Sp(x)$ is the Spence or dilog function, $Sp(x) = - \int_0^1 \frac{dt}{t} \ln(1 - xt)$ with $Sp(1) = \pi^2/6$. In the high energy limit, $\frac{E_{thr}}{E} \rightarrow 1$, we recover the result of Ref.[15]. For the details, we address the reader to the Appendix. This $\ln^2 \left(\frac{-t}{m^2} \right)$ factor serves as the justification of the QRCS approximation. The full result may be represented as a “Taylor expansion” in powers of $\ln \left(\frac{-t}{m^2} \right) \sim 10$. By studying the QRCS approximation we show in a model independent way that the leading term in this expansion is quadratic. Since this leading term is large, we can (under certain kinematical conditions) neglect further terms.

The RCS tensor may be taken for instance in the basis of Prange [18] or, equivalently of Berg and Lindner [19],

$$\begin{aligned} W_{RCS}^{\mu\nu} &= \bar{N}' \left\{ \frac{P'^\mu P'^\nu}{P'^2} (B_1 + \cancel{K}B_2) + \frac{n^\mu n^\nu}{n^2} (B_3 + \cancel{K}B_4) \right. \\ &+ \frac{P'^\mu n^\nu - n^\mu P'^\nu}{P'^2 n^2} i\gamma_5 B_7 \\ &\left. + \frac{P'^\mu n^\nu + n^\mu P'^\nu}{P'^2 n^2} \not{n} B_6 \right\} N, \end{aligned} \quad (17)$$

with the vectors defined as $P' = P - \frac{P \cdot K}{K^2} K$, $n^\mu = \varepsilon^{\mu\nu\alpha\beta} P_\nu K_\alpha q_\beta$ such that $P' \cdot K = P' \cdot n = n \cdot K = 0$. The amplitudes B_i are functions of ν and t . This form of Compton tensor is convenient due to the simple form of the tensors appearing in Eq. (17).

Before contracting the leptonic and hadronic tensors, we notice that the amplitude B_7 can only contribute to the invariant amplitude \tilde{F}_6 , since it contains the $\bar{N}'\gamma_5 N$ structure. \tilde{F}_6 does not contribute at leading order in m to neither observable of interest, therefore B_7 will be neglected in the following. The remaining tensors in Eq.(17) are symmetric in indices $\mu\nu$.

$$\text{Im} \mathcal{M}_{2\gamma}^{QRCS} = e^2 m I_0 \bar{u}' u W_{RCS}^{\mu\nu} g_{\mu\nu}. \quad (18)$$

Finally, we identify different terms in Eq. (18) with the structures, together with amplitudes $\tilde{F}_{1,\dots,6}$ parametrizing elastic ep -scattering amplitude in Eqs. (3,4) and find for the invariant amplitudes for the elastic electron-proton scattering in the QRCS approximation:

$$\text{Im} \tilde{G}_M^{QRCS} = \text{Im} \tilde{F}_2^{QRCS} = \text{Im} \tilde{F}_3^{QRCS} = 0 \quad (19)$$

$$\text{Im} \tilde{F}_4^{QRCS} = -M t I_0 \text{Im}(B_1 + B_3) \quad (20)$$

$$\text{Im} \tilde{F}_5^{QRCS} = -M^2 t I_0 \text{Im}(B_2 + B_4) \quad (21)$$

B_n :

We obtain for B_n in the QRCS approximation:

$$B_n = mtI_0\sqrt{2\varepsilon(1-\varepsilon)}\sqrt{1+\tau}(\tau G_M^2 + \varepsilon G_E^2)^{-1} \cdot \{G_E \text{Im}(B_1 + B_3) + \nu F_1 \text{Im}(B_2 + B_4)\}. \quad (22)$$

The result of Eq.(22) is obtained by only using the assumption that the QRCS kinematics dominate the integral in Eq.(10). The combinations of the RCS amplitudes appearing in the final result can be furthermore expressed in terms of the helicity amplitudes of real Compton scattering. With these latter defined as $T_{\lambda'_\gamma \lambda'_N, \lambda_\gamma \lambda_N} \equiv \varepsilon_{\lambda'_\gamma}^{\nu*} \varepsilon_{\lambda'_N}^\mu W_{\mu\nu}^{RCS}$, one has [20, 22]:

$$B_1 + B_3 = -\frac{1}{\sqrt{-t}} \left(T_{-1-\frac{1}{2}, 1\frac{1}{2}} + T_{1-\frac{1}{2}, -1\frac{1}{2}} \right) - \frac{2M}{M^4 - su} T_{1\frac{1}{2}, -1\frac{1}{2}} \quad (23)$$

$$B_2 + B_4 = \frac{2M}{s - M^2} \frac{1}{\sqrt{-t}} \left(T_{-1-\frac{1}{2}, 1\frac{1}{2}} + T_{1-\frac{1}{2}, -1\frac{1}{2}} \right) + \frac{2}{M^4 - su} \frac{s + M^2}{s - M^2} T_{1\frac{1}{2}, -1\frac{1}{2}} \quad (24)$$

As can be seen, only photon helicity-flipping amplitudes enter the final result for B_n in the QRCS approximation. This is the main result of this work.

V. RESULTS

In this section, we consider the impact of the QRCS contributions onto the beam normal spin asymmetry in different kinematics: low energies (πN intermediate states), high energies and forward angles, i.e. Regge regime (2π exchange in the t -channel) and hard regime (handbag diagrams and two gluon exchange).

A. Low energies: πN multipoles

Above the pion production threshold, the imaginary part of the RCS helicity amplitudes can be related to the pion photo- and electro-production multipoles. These relations read [20, 22] for the three amplitudes entering

$$\begin{aligned} \text{Im}T_{-1-\frac{1}{2}, 1\frac{1}{2}} &= \sin \frac{\Theta}{2} 16\pi q_\pi \sqrt{s} \sum_{k \geq 0} (k+1)^2 \\ &\times [|A_{k+}|^2 - |A_{(k+1)-}|^2] \\ &\times F(-k, k+2, 2, \sin^2 \frac{\Theta}{2}) \end{aligned} \quad (25)$$

$$\begin{aligned} \text{Im}T_{1-\frac{1}{2}, -1\frac{1}{2}} &= -\sin^3 \frac{\Theta}{2} 8\pi q_\pi \sqrt{s} \sum_{k \geq 1} \frac{k^2(k+1)^2(k+2)^2}{12} \\ &\times [|B_{k+}|^2 - |B_{(k+1)-}|^2] \\ &\times F(-k+1, k+3, 4, \sin^2 \frac{\Theta}{2}) \end{aligned} \quad (26)$$

$$\begin{aligned} \text{Im}T_{1\frac{1}{2}, -1\frac{1}{2}} &= \sin^2 \frac{\Theta}{2} \cos \frac{\Theta}{2} 8\pi q_\pi \sqrt{s} \sum_{k \geq 1} \frac{k(k+1)^2(k+2)}{2} \\ &\times \text{Re} \left[B_{k+} A_{k+}^* - B_{(k+1)-} A_{(k+1)-}^* \right] \\ &\times F(-k+1, k+3, 3, \sin^2 \frac{\Theta}{2}), \end{aligned} \quad (27)$$

where q_π is the c.m. pion three-momentum and the hypergeometric function is defined as

$$F(a, b, c, x) = 1 + \frac{ab}{c} \frac{x}{1!} + \frac{a(a+1)b(b+1)}{c(c+1)} \frac{x^2}{2!} + \dots \quad (28)$$

We keep only few first multipoles in this infinite series, namely A_{0+} , A_{1+} , B_{1+} , A_{2-} , B_{2-} which obtain their leading contributions from threshold pion production, $\Delta(1232)$ and $D_{13}(1520)$ resonances. The result for B_n reads:

$$\begin{aligned} B_n = -8\pi mq_\pi \frac{st^2}{(s - M^2)^2} I_0 \frac{\sqrt{2\varepsilon(1-\varepsilon)}\sqrt{1+\tau}}{\tau G_M^2 + \varepsilon G_E^2} \\ \cdot \left\{ \left(\frac{E_{lab}}{M} F_2 - F_1 \right) \right. \\ \cdot [|A_{0+}|^2 - |A_{1-}|^2 + 4(|A_{1+}|^2 - |A_{2-}|^2)] \\ - \frac{6\sqrt{s}}{M} F_1 \text{Re} (B_{1+} A_{1+}^* - B_{2-} A_{2-}^*) \\ - \frac{3}{2} \sin^2 \frac{\Theta}{2} \left[\left(\frac{E_{lab}}{M} F_2 - F_1 \right) \right. \\ \cdot (4(|A_{1+}|^2 - |A_{2-}|^2) + |B_{1+}|^2 - |B_{2-}|^2) \\ + 2 \left(\frac{k}{M} F_2 - \frac{E}{M} F_1 \right) \\ \cdot \text{Re} (B_{1+} A_{1+}^* - B_{2-} A_{2-}^*) \left. \right] \left. \right\}. \end{aligned} \quad (29)$$

The helicity multipoles are related to the electromagnetic multipoles $E_{l+, (l+1)-}$, $M_{l+, (l+1)-}$ as

$$E_{0+} = A_{0+}, \quad M_{1-} = A_{1-}, \quad (30)$$

and for $l \geq 1$

$$\begin{aligned} E_{l+} &= \frac{1}{l+1} \left[A_{l+} + \frac{l}{2} B_{l+} \right] \\ M_{l+} &= \frac{1}{l+1} \left[A_{l+} - \frac{l+2}{2} B_{l+} \right] \\ E_{(l+1)-} &= -\frac{1}{l+1} \left[A_{(l+1)-} - \frac{l+2}{2} B_{(l+1)-} \right] \\ M_{(l+1)-} &= -\frac{1}{l+1} \left[A_{(l+1)-} + \frac{l}{2} B_{(l+1)-} \right] \end{aligned} \quad (31)$$

It is informative to consider the contributions of E_{0+} and M_{1+} which are dominant at low energies. Neglecting other multipoles, we get:

$$\begin{aligned} B_n = -8\pi mq_\pi \frac{st^2}{(s-M^2)^2} I_0 \frac{\sqrt{2\varepsilon(1-\varepsilon)}\sqrt{1+\tau}}{\tau G_M^2 + \varepsilon G_E^2} \\ \cdot \left\{ \left(\frac{E_{lab}}{M} F_2 - F_1 \right) [|E_{0+}|^2 + |M_{1+}|^2] \right. \\ \left. + \left(\frac{3\sqrt{s}}{M} F_1 + 3 \sin^2 \frac{\Theta}{2} \frac{(\sqrt{s}-M)^2}{2\sqrt{s}M} \left[\frac{\sqrt{s}+M}{M} F_2 - F_1 \right] \right) \right. \\ \left. \cdot |M_{1+}|^2 \right\}. \end{aligned} \quad (32)$$

The first term in the brackets is negative for $E_{lab} \leq \frac{M}{\kappa} \approx 0.45$ GeV for the proton target, and always negative for the neutron target. Due to the overall minus sign, the beam normal spin asymmetry necessarily obtains a positive contribution from the threshold pion production. Moving towards the $\Delta(1232)$ resonance position, we see that the dominant contribution now comes from the second term. The factor multiplying the $|M_{1+}|^2$ term is always positive for the proton and negative for the neutron. Therefore one expects that the Δ resonance give a large negative contribution to B_n on the proton target, and a positive one on the neutron target. We use the MAID2003 multipoles as input to Eq.(29) and present in Fig. 3 the energy dependence of the beam normal spin asymmetry for the proton target over the resonance region. This result can be compared to the results of Refs.[10, 12]. If confronted to the full calculation [10], we find agreement with their findings in the QRCS approximation. In Ref. [12], the authors do nominally the same approximation as we do, keeping the $\ln^2(Q^2/m^2)$ and the RCS part of the hadronic tensor only but arrive to the same sign of the contributions of the E_{0+} and M_{1+} multipoles for the proton. They are furthermore able to describe both low energy backward angle data from SAMPLE and intermediate energy and angle data from MAMI within the same approximation. It has been shown in [10] that the QRCS approximation does work well at backward angles (in the sense that it represents the dominant part of the full integration range) but drops short at forward angles, where the exchange of at least one hard virtual photon is important (for very forward angles, see [15]). Therefore, even if the QRCS approximation did work in the forward regime, one should not take

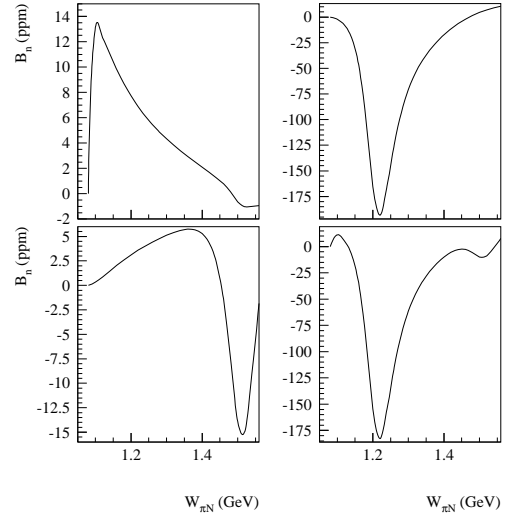


FIG. 3: Beam normal spin asymmetry for the reaction $\vec{e} + p \rightarrow e + p$ in the QRCS approximation at fixed c.m. scattering angle $\Theta_{cm} = 120^\circ$ as function of the πN invariant mass $W_{\pi N}$. The contribution of the E_{0+} multipole (upper left panel), E_{1+} and M_{1+} (upper right panel), E_{2-} and M_{2-} (lower left panel) are shown separately. The full result within the QRCS approximation is shown in the lower right panel.

this success too seriously, since the neglected double or single virtual Compton scattering effects are important. We show the angular distributions of B_n on the proton target for different values of the electron *lab* energy in Fig. 4. In Fig. 5, we display the energy distributions of B_n on the neutron over the resonance region.

It is necessary to note that the resonance region does not seem to be favorable for the QRCS approximation. In this approximation, the value of the hadronic amplitude is taken at the largest energy available and is not integrated over the full spectrum. Therefore, if one goes above a resonance position, it is only tail of the resonance that contribute, which causes the asymmetry to drop quite fast (see the sharp resonance behaviour at $\Delta(1232)$, $D_{13}(1520)$ in Fig.3). In a full calculation, also intermediate energies of the hadronic system do contribute and the asymmetry does not have such a sharp energy dependence. So, it is preferable to use the QRCS approximation in the region where the energy dependence is rather smooth. Furthermore, the quality of the QRCS approximation is function of the scattering angle, as well. It works better at backward angles and worse at forward angles. The reason for this is clear: taking the limit of the soft intermediate electron, $k_1 \approx 0$ and neglecting the dependence of the hadronic and leptonic tensors on k_1 corresponds to performing Taylor expansion of the integration result in powers of $\ln \frac{Q^2}{m^2}$ and neglecting all the terms beyond the first leading log term $\sim \ln^2 \frac{Q^2}{m^2}$. The

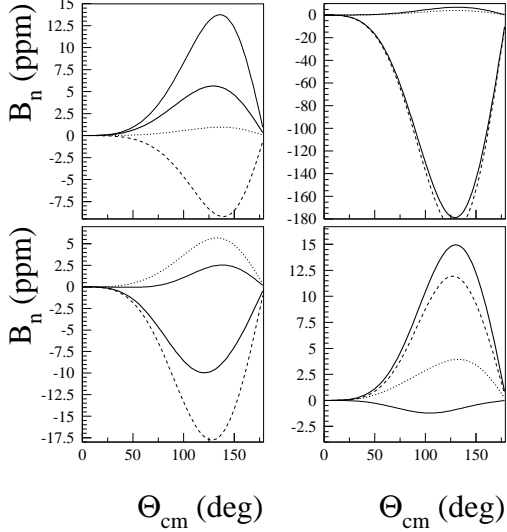


FIG. 4: Beam normal spin asymmetry on the proton as function of c.m. scattering angle at different values of *lab* energy: 200 MeV (upper left panel), 300 MeV (upper right panel), 570 MeV (lower left panel) and 855 MeV (lower right panel). The different lines represent E_{0+} multipole contribution (thin solid lines), E_{1+} and M_{1+} contribution (dashed lines), E_{2-} and M_{2-} contribution (dotted lines), and the sum of all (thick solid lines)

larger Q^2 , the better the approximation works. This behaviour was first observed in Ref.[10]. Instead, results of Ref.[12] suggest that the loop integral in B_n is completely dominated by the QRCS region in all the kinematics (backward regime for SAMPLE data and rather forward regime for MAMI data).

B. Regge regime: 2π exchange

The calculation of Ref. [17] estimates B_n as

$$B_n \sim \sigma_{tot} \ln(-t/m^2), \quad (33)$$

which is based on taking the RCS amplitude in the exact forward limit. If one allows the momentum transfer to be non-zero, one however obtains the contribution from photon helicity flip amplitudes, which is the result of this work. Though it is logical to expect that these amplitudes be suppressed at low values of t , there is a competing factor of $\sim \ln^2 \frac{Q^2}{m^2}$, which can be of the order of several hundreds. In this subsection, we provide an estimate of such a contribution at forward kinematics. The combinations of the RCS amplitudes $B_1 + B_3$, $B_2 + B_4$ in Regge regime are known to have the quantum numbers of a scalar isoscalar exchange in the t -channel which was successfully described by σ -meson [20] or equivalently, by two pion exchange in the t -channel [21]. Since the

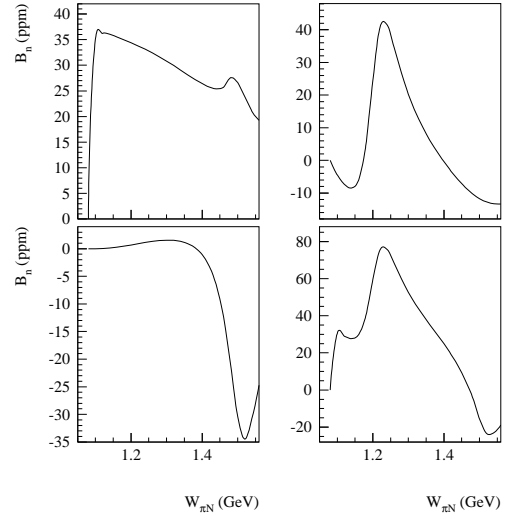


FIG. 5: Beam normal spin asymmetry for the reaction $\vec{e} + n \rightarrow e + n$ in the QRCS approximation as function of the πN invariant mass $W_{\pi N}$. Notation as in Fig. 3

effective σ -meson exchange does not result in a non-zero imaginary part in the s -channel, one should use the two pion exchange mechanism accompanied by multiparticle intermediate state in the s -channel. In this section we estimate $B_1 + B_3$ and $B_2 + B_4$ through πN and ρN intermediate states contributions within the “minimal” Regge model for π and ρ photoproduction [25] where reggeized description of high energy pion production is obtained by adding the t -channel meson exchange amplitude and (in the case of γp reaction) s -channel Born amplitude which is necessary to ensure gauge invariance. The reggeization procedure naturally leads to the substitution of each t -channel Feynman propagator by its Regge counterpart, $\frac{1}{t - m_\pi^2} \rightarrow \mathcal{P}_\pi^R(\alpha_\pi(t))$, with

$$\mathcal{P}_\pi^R = \left(\frac{s}{s_0} \right)^{\alpha_\pi(t)} \frac{\pi \alpha'_\pi}{\sin \pi \alpha_\pi(t)} \frac{1}{\Gamma(1 + \alpha_\pi(t))}, \quad (34)$$

with $\alpha_\pi(t) = \alpha'_\pi(t - m_\pi^2)$ and $\alpha'_\pi = 0.7 \text{ GeV}^{-2}$. Gauge invariance requires the s -channel piece to be reggeized in the same way, i.e., to be multiplied by $(t - m_\pi^2) \mathcal{P}_\pi^R(\alpha_\pi(t))$. For compactness, we will use the shorthand [20],

$$A_1 \equiv \frac{1}{t} [B_1 + B_2 + \nu(B_2 + B_4)] \quad (35)$$

for the combination of the B_i ’s which enters the result for the asymmetry. Here, we list the results of the calculation

of A_1 :

$$\text{Im}A_1^{\pi N} = \frac{2m_\pi^2 C_\pi^2}{M(s - M^2)} (B_0^\pi - M^2 A_0^\pi), \quad (36)$$

$$\begin{aligned} \text{Im}A_1^{\rho N} &= \frac{m_\rho^2 C_\rho^2}{2M(s - M^2)} \left\{ \frac{M^2}{s - M^2} C_0^\rho \right. \\ &\quad \left. + \frac{s - 3M^2 + 5m_\rho^2}{2} B_0^\rho + m_\rho^2 \frac{s + M^2}{2} A_0^\rho \right\}, \end{aligned}$$

where $C_\pi = 2\sqrt{2}Me^{\frac{f_{\pi NN}}{m_\pi}}$ with $f_{\pi NN}^2/4\pi = 0.08$, and $C_\rho = 2\sqrt{2}Me^{\frac{f_{\pi NN}}{m_\pi} \frac{f_{\rho\pi\gamma}}{m_\pi}}$ with $f_{\rho\pi\gamma} = 0.103$ [25]. Where possible, m_π and Q^2 were neglected as compared to s , M , m_ρ in order to simplify the final expression. The scalar integrals A_0 , B_0 , C_0 for both πN and ρN contributions are given in the Appendix.

The result of Eq.(36) leads to negligibly small contribution to the B_n , of the order of 10^{-2} ppm for energies between 6 and 45 GeV, which is to be compared to ≈ 5 ppm from Ref. [17]. There are three suppression factors which are responsible for this small result. Firstly, the Reggeization procedure which leads to suppression in energy $\nu^{\alpha\pi(t)}$. Secondly, the amplitude A_1 is defined as the combination $\frac{1}{-t}[B_1 + B_3 + \nu(B_2 + B_4)]$, and the singularity $\frac{1}{t}$ in the definition only cancels if taking the gauge invariant combination as described in [25]. Therefore, we obtain an additional suppression factor of t . The other feature of the result of Eqs.(36,37) is that both contributions are suppressed by factors $\frac{m_\pi^2}{s - M^2}$ and $\frac{m_\rho^2}{s - M^2}$, respectively. In the case of the pion, it is interesting to observe this fact in view of somewhat surprising success of the effective field description of the SAMPLE data point on B_n without pion contribution. This might give a hint that the pion contribution to B_n at low energies is suppressed by the pion mass, if calculated to the same order.

C. Hard regime: GPD's

Recently, beam normal spin asymmetry was studied in the hard scattering regime [14] in the framework of the handbag mechanism. In this picture, the process factorizes into the hard part (electron scattering off an on-shell quark with the exchange of two spacelike photons) and the soft part which is parametrized by the generalized parton distributions (GPD's). However, one cannot access the QRCS kinematics here, since it is impossible for an on-shell quark to absorb (emit) a hard real photon and remain on-shell. As it has been noticed before, the QRCS kinematics selects the RCS amplitudes with the photon helicity flip, i.e. the helicity changes by two units. In the context of the GPD's, helicity amplitudes with the helicity changed by 2 units were considered in several works. In the collinear kinematics, this requires that scattering occurs on a parton of spin 1, that is gluon. The corresponding gluon helicity flip GPD's were introduced in

[28]

$$\begin{aligned} &\frac{1}{x} \int \frac{d\lambda}{2\pi} e^{i\lambda x} \langle p' S' | F^{(\mu\alpha}(-\frac{\lambda}{2}n) F^{\nu\beta)}(-\frac{\lambda}{2}n) | p S \rangle \\ &= H_{T_g}(x, \xi) \bar{N}'(p', S') \frac{P^{([\mu} q^{\alpha]} i\sigma^{\nu\beta)}}{M} N(p, S) \\ &\quad + E_{T_g}(x, \xi) \bar{N}'(p', S') \frac{P^{([\mu} q^{\alpha]} \gamma^{[\nu} q^{\beta]})}{M^2} N(p, S) \quad (37) \end{aligned}$$

where $H_{T_g}(x, \xi)$, $E_{T_g}(x, \xi)$ are the double helicity flip gluon GPD's, $q = p' - p$, and the matrix element is taken between the initial and final nucleon states with the momenta p and p' , and spins S and S' , respectively. The integration is performed along the light-cone vector $n^\mu = (1, 0, 0, 1)$. x and ξ are the longitudinal parton momentum fraction and skewness parameter, respectively. Furthermore, $[\mu\alpha]$ and $[\nu\beta]$ are antisymmetric pairs of indices, while (\dots) means symmetrization and removal of the trace. These operations are essential since the product of operators must transform as irreducible representations of the Lorentz group. This requirement rules out the possibility to see these GPD's in the QRCS kinematics, since it is exactly the trace of the RCS tensor that contributes to B_n in the QRCS regime, c.f. Eq.(18). So, our conclusion is that in the QRCS kinematics, contributions from generalized parton distributions are ruled out.

VI. SUMMARY

In summary, we presented a calculation of the beam normal spin asymmetry. This observable obtains its leading contribution from the imaginary part of the two photon exchange graph times the Born amplitude and is directly related to the imaginary part of doubly virtual Compton scattering. The resulting loop integral obtains a large contribution from the kinematics when both exchanged photons are nearly real and collinear to the external electrons. We adopt the QRCS or equivalent photons approximation which allows to take the hadronic part out of the integral and to perform the integration over the electron phase space analytically. For the hadronic part, we use the full real Compton scattering amplitude and show, that only photon helicity flipping amplitudes contribute in this observable in the QRCS approximation. At low energies, we relate this helicity flipping Compton amplitude to the πN multipoles and discuss the contributions of different multipoles.

At high energies and forward scattering angles (Regge regime), we provide an explicit calculation which is due to two pion exchange in the t -channel. The resulting values of the asymmetry are of the order 10^{-2} ppm for the energies in the range 6 – 45 GeV. We conclude that the double logarithmic enhancement does not dominate B_n in forward regime since it comes with helicity-flip Compton amplitude which highly suppresses this behaviour.

Finally, we consider possible contributions to B_n in the hard kinematics, among which contributions from quark

and gluon GPD's and show that such contributions are ruled out in the QRCS kinematics.

Acknowledgments

The author is grateful to Prof. M.M.Giannini for continuous support and to Dr. M.J. Ramsey-Musolf and D. O'Connell for numerous discussions and for thorough reading of the manuscript. The work was supported by Italian MIUR and INFN, and by US Department of Energy Contract DE-FG02-05ER41361.

VII. APPENDIX A: INTEGRALS OVER ELECTRON PHASE SPACE

In this section we present calculation of the integrals over electron phase space appearing in the QRCS approximation. First we calculate the scalar integral I_0 ,

$$I_0 = \int_0^{k_{thr}} \frac{k_1^2 dk_1}{2E_1(2\pi^3)} \int \frac{d\Omega_{k_1}}{(k - k_1)^2(k' - k_1)^2}, \quad (38)$$

where the upper integration limit k_{thr} corresponds to the inelastic threshold (i.e. pion production), $k_{thr} = \sqrt{\frac{(s - (M + m_p i)^2)^2}{4s}} - m^2$. We next introduce integration over the Feynman parameter $\frac{1}{ab} = \int_0^1 \frac{dx}{[a + (b - a)x]^2}$. We chose the polar axis such as $\vec{k}_1 \cdot (\vec{k} - x\vec{q}) = k_1 |\vec{k} - x\vec{q}| \cos \Theta_1$ with $|\vec{k} - x\vec{q}|^2 = k^2 + x(1 - x)t$ and perform angular integration. We furthermore change integration over dk_1 to integration over dimensionless $z = E_1/E$

$$I_0 = \frac{1}{-8\pi^2 t} \int_{\frac{m}{E}}^{\frac{E_{thr}}{E}} \frac{dz}{\sqrt{z^2 - \frac{m^2}{E^2} - \frac{4m^2}{t}(1-z)^2}} \cdot \ln \frac{\sqrt{z^2 - \frac{m^2}{E^2} - \frac{4m^2}{t}(1-z)^2} + \sqrt{z^2 - \frac{m^2}{E^2}}}{\sqrt{z^2 - \frac{m^2}{E^2} - \frac{4m^2}{t}(1-z)^2} - \sqrt{z^2 - \frac{m^2}{E^2}}}, \quad (39)$$

To perform the integration over the electron energy, we follow here the main details of the calculation in Appendix A of Ref.[15]. The result reads

$$I_0 = \frac{1}{-32\pi^2 t} \left\{ \ln^2 \left(\frac{-t}{m^2} \frac{E_{thr}^2}{E^2} \right) + 8Sp \left(\frac{E_{thr}}{E} \right) \right\}, \quad (40)$$

where $Sp(x)$ is the Spence or dilog function, $Sp(x) = -\int_0^1 \frac{dt}{t} \ln(1 - xt)$ with $Sp(1) = \pi^2/6$. In the high energy limit, $\frac{E_{thr}}{E} \rightarrow 1$, we recover the result of Ref.[15].

VIII. APPENDIX B: SCALAR INTEGRALS FOR HELICITY FLIP AMPLITUDE

The vector and tensor integrals can be reduced to the scalar ones by means of standard methods [27]. The remaining integrals to be calculated are the two, three, and

four-point scalar integrals. Here we are only interested in the imaginary part of these, therefore there are only three integrals with non-zero imaginary part: the two-point integral

$$\begin{aligned} C_0^\pi &= \text{Im} \int \frac{d^4 p_\pi}{(2\pi)^4} \frac{1}{p_\pi^2 - m_\pi^2} \frac{1}{(P + K - p_\pi)^2 - M^2} \\ &= \frac{1}{8\pi} \frac{|\vec{p}_\pi|}{\sqrt{s}}, \end{aligned} \quad (41)$$

with $|\vec{p}_\pi| = \sqrt{\frac{(s - M^2 + m_\pi^2)^2}{4s} - m_\pi^2}$; the three-point one

$$\begin{aligned} B_0^\pi &= \text{Im} \int \frac{d^4 p_\pi}{(2\pi)^4} \frac{1}{p_\pi^2 - m_\pi^2} \frac{1}{(k - p_\pi)^2 - m_\pi^2} \\ &\quad \cdot \frac{1}{(P + K - p_\pi)^2 - M^2} \\ &= -\frac{1}{8\pi(s - M^2)} \ln \frac{2E_\pi}{m_\pi}, \end{aligned} \quad (42)$$

and finally, the four-point integral:

$$\begin{aligned} A_0^\pi &= \text{Im} \int \frac{d^4 p_\pi}{(2\pi)^4} \frac{1}{(k - p_\pi)^2 - m_\pi^2} \frac{1}{p_\pi^2 - m_\pi^2} \\ &\quad \cdot \frac{1}{(k' - p_\pi)^2 - m_\pi^2} \frac{1}{(P + K - p_\pi)^2 - M^2} \\ &= \frac{1}{8\pi Q^2(s - M^2 + m_\pi^2)} \\ &\quad \cdot \frac{1}{\sqrt{1 + \frac{4m_\pi^2 E^2}{Q^2 p_\pi^2}}} \ln \frac{\sqrt{1 + \frac{4m_\pi^2 E^2}{Q^2 p_\pi^2}} + 1}{\sqrt{1 + \frac{4m_\pi^2 E^2}{Q^2 p_\pi^2}} - 1}. \end{aligned} \quad (43)$$

These integrals should however be reggeized as described in Section V by substituting the Regge propagator instead of the Feynman one. Denoting $t_1 = (k - p_\pi)^2$ and $t_2 = (k' - p_\pi)^2$ the momentum transferred by the pions in the t -channel, we have for the reggeized version of scalar integrals:

$$\begin{aligned} (C_0^\pi)^R &= \frac{1}{32\pi^2} \frac{p_\pi}{\sqrt{s}} \int d\Omega_\pi (t_1 - m_\pi^2) \mathcal{P}_\pi^R(\alpha_\pi(t_1)) \\ &\quad \cdot (t_2 - m_\pi^2) \mathcal{P}_\pi^R(\alpha_\pi(t_2)) \end{aligned} \quad (44)$$

$$\begin{aligned} (B_0^\pi)^R &= \frac{1}{32\pi^2} \frac{p_\pi}{\sqrt{s}} \int d\Omega_\pi (t_1 - m_\pi^2) \\ &\quad \mathcal{P}_\pi^R(\alpha_\pi(t_1)) \mathcal{P}_\pi^R(\alpha_\pi(t_2)), \end{aligned} \quad (45)$$

$$(A_0^\pi)^R = \frac{1}{32\pi^2} \frac{p_\pi}{\sqrt{s}} \int d\Omega_\pi \mathcal{P}_\pi^R(\alpha_\pi(t_1)) \mathcal{P}_\pi^R(\alpha_\pi(t_2)) \quad (46)$$

Similarly, in the case of the ρ -exchange in the s -channel, the integrals with non-zero imaginary part are:

$$\begin{aligned} C_0^\rho &= \text{Im} \int \frac{d^4 p_\rho}{(2\pi)^4} \frac{1}{p_\rho^2 - m_\rho^2} \frac{1}{(P + K - p_\rho)^2 - M^2} \\ &= \frac{1}{8\pi} \frac{|\vec{p}_\rho|}{\sqrt{s}}, \end{aligned}$$

$$\begin{aligned}
B_0^\rho &= \text{Im} \int \frac{d^4 p_\rho}{(2\pi)^4} \frac{1}{p_\rho^2 - m_\rho^2} \frac{1}{(k - p_\rho)^2 - m_\pi^2} \\
&\quad \cdot \frac{1}{(P + K - p_\rho)^2 - M^2} \\
&= -\frac{1}{8\pi(s - M^2)} \ln \frac{2E_\rho(s - M^2)}{Mm_\rho^2},
\end{aligned}$$

$$\begin{aligned}
A_0^\rho &= \text{Im} \int \frac{d^4 p_\rho}{(2\pi)^4} \frac{1}{(k - p_\rho)^2 - m_\pi^2} \frac{1}{p_\rho^2 - m_\rho^2} \\
&\quad \cdot \frac{1}{(k' - p_\rho)^2 - m_\pi^2} \frac{1}{(P + K - p_\rho)^2 - M^2} \\
&= \frac{1}{8\pi Q^2(s - M^2 + m_\rho^2)} \frac{1}{\sqrt{1 + \frac{4\sigma^2}{Q^2 p_\rho^2}}} \\
&\quad \cdot \ln \frac{\sqrt{1 + \frac{4\sigma^2}{Q^2 p_\rho^2}} + 1}{\sqrt{1 + \frac{4\sigma^2}{Q^2 p_\rho^2}} - 1}, \tag{47}
\end{aligned}$$

with $|\vec{p}_\rho| = \sqrt{\frac{(s - M^2 + m_\rho^2)^2}{4s} - m_\rho^2}$, and $\sigma^2 = E^2 m_\rho^2 - EE_\rho(m_\rho^2 - m_\pi^2) + \frac{1}{4}(m_\rho^2 - m_\pi^2)^2$. If neglecting the pion mass, $\sigma = \frac{Mm_\rho^2}{2s}$. The reggeization procedure is the same as for πN - intermediate state.

[1] M.K. Jones *et al.*, Phys. Rev. Lett. **84** (2000) 1398; O. Gayou *et al.*, Phys. Rev. Lett. **88** (2002) 092301.

[2] L. Andivahis *et al.*, Phys. Rev. **D 50** (1994) 5491; M.E. Christy *et al.*, Phys. Rev. **C 70** (2004) 015206; I.A. Qattan *et al.*, Phys. Rev. Lett. **94** (2005) 142301, [arXiv:nucl-ex/0410010].

[3] P.A.M. Guichon, M. Vanderhaeghen, Phys. Rev. Lett. **91** (2003) 142303.

[4] L.W. Mo and Y.S. Tsai, Rev. Mod. Phys. **41** (1969) 205; L.C. Maximon and J.A. Tjon, Phys. Rev. **C 62** (2000) 054320.

[5] P.G. Blunden, W. Melnitchouk and J.A. Tjon, Phys. Rev. Lett. **91** (2003) 142304.

[6] Y.C. Chen, A. Afanasev, S.J. Brodsky, C.E. Carlson and M. Vanderhaeghen, Phys. Rev. Lett. **93** (2004) 122301.

[7] N.F. Mott, Proc. R. Soc. London, Ser. **A135** (1935) 429; A.O. Barut and C. Fronsdal, Phys. Rev. **120** (1960) 1871; A. De Rujula, J.M. Kaplan and E. De Rafael, Nucl. Phys. **B 35** (1971) 365.

[8] S.P. Wells *et al.* [SAMPLE Collaboration], Phys. Rev. **C 63** (2001) 064001; F. Maas *et al.* [MAMI A4 Collaboration], Phys. Rev. Lett. **94** (2005) 082001.

[9] A. Afanasev, I. Akushevich and N.P. Merenkov, [arXiv:hep-ph/0208260].

[10] B. Pasquini and M. Vanderhaeghen, Phys. Rev. **C 70** (2004) 045206.

[11] L. Diaconescu and M.J. Ramsey-Musolf, Phys. Rev. **C 70** (2004) 054003.

[12] D. Borisyuk and A. Kobushkin, nucl-th/0508053.

[13] SLAC E158 Experiment, contact person K. Kumar, G. Cates, K. Kumar and D. Lhuillier, spokespersons HAPPEX-2 Experiment, JLab E-99-115; D. Beck, spokesperson JLab/G0 Experiment, JLabE-00—6, E-01-116.

[14] M. Gorchtein, P.A.M. Guichon and M. Vanderhaeghen, Nucl. Phys. **A 741** (2004) 234.

[15] A.V. Afanasev, N.P. Merenkov, Phys. Lett. **B 599** (2004) 48; Phys. Rev. **D 70** (2004) 073002.

[16] M. Gorchtein, hep-ph/0505022.

[17] A.V. Afanasev, N.P. Merenkov, hep-ph/0407167 v2.

[18] R.E. Prange, Phys. Rev. **110** (1958) 240.

[19] R.A. Berg and C.N. Lindner, Nucl. Phys. **26** (1961) 259.

[20] A.I. L'vov, V.A. Petrun'kin, M. Schumacher, Phys. Rev. **C 55** (1997) 359.

[21] D. Drechsel, M. Gorchtein, B. Pasquini, M. Vanderhaeghen, Phys. Rev. **C 61** (1999) 015204.

[22] B. Pasquini, M. Gorchtein, D. Drechsel, A. Metz, M. Vanderhaeghen, Eur. Phys. **A 11** (2001) 185.

[23] M. Gorchtein, PhD thesis, Universität Mainz.

[24] T.H. Bauer, R.D. Spital, D.R. Yennie and F.M. Pipkin, Rev. Mod. Phys. **50** (1978) 261; [Erratum-ibid. **51** (1979) 407].

[25] M. Guidal, J.-M. Laget, M. Vanderhaeghen, Nucl. Phys. **A 627** (1997) 645.

[26] A. Metz and D. Drechsel, Z. Phys. **A 356** (1996) 351; A. Metz, PhD Thesis, Universität Mainz.

[27] G. Passarino and M. Veltman, Nucl. Phys. **B160** (1979) 151.

[28] P. Hoodbhoy and X. Ji, Phys. Rev. **D 58** (1998) 054006; N. Kivel, L. Mankiewicz and M.V. Polyakov, Phys. Lett. **B 467** (1999) 263-270; A.V. Belitsky and D. Müller, Phys. Lett. **B 486** (2000) 369-377.